Phys. Status Solidi B **251,** No. 11, 2185–2188 (2014) / **DOI** 10.1002/pssb.201400025

physica status solidi b
www.pss-b.com
basic solid state physics

An atomistic picture of the diffusion of two vacancies forming a di-vacancy in Si

Eiji Kamiyama[*,1], **Koji Sueoka**[**,1], **and Jan Vanhellemont**[***,2]

[1] Department of Communication Engineering, Okayama Prefectural University, 111 Kuboki, Soja, Okayama 719-1197, Japan
[2] Department of Solid State Sciences, Ghent University, Krijgslaan 281-S1, 9000 Gent, Belgium

Received 26 April 2014, revised 4 June 2014, accepted 5 June 2014
Published online 9 September 2014

Keywords capture cross-section, continuum model, diffusion, di-vacancy, formation, molecular dynamics, silicon

[*] Corresponding author: e-mail ejkamiyama@aol.com, Phone: +81 866 94 2136, Fax: +81 866 94 2199
[**] e-mail sueoka@c.oka-pu.ac.jp, Phone: +81 866 94 2136, Fax: +81 866 94 2199
[***] e-mail jan.vanhellemont@ugent.be, Phone: +32 499 593857, Fax: +32 9 2644996

A method is proposed to calculate the formation of a point defect pair in Si based on an atomistic picture. As an illustration, the capturing of a vacancy (V) by another V forming a di-vacancy is described semi-quantitatively. It is shown that in Si, the number of most likely diffusion paths of two vacancies V to form a di-vacancy is limited. The energetically most favorable diffusion paths are the twelve zigzag Si chains surrounding the V along the ⟨110⟩ directions. Systematically calculating all of the irreducible configurations of two vacancies, each with its weight (=total number of each possible configuration), enables determining all possible V diffusion paths with their relative weights. This obtained picture is different from diffusion in the continuum model, which does not take into account the anisotropy of covalent bonds in the diamond lattice. The proposed approach is a first step towards the calculation of the effective "capture cross-section" for the formation of point defect pairs that can be used in continuum models.

1 Introduction An as-grown Si crystal can contain many types of clusters of point defects, which can have an important impact on material and device properties. A well-known example is grown-in voids consisting of vacancies [1–3]. Each Si atom is connected by four covalent bonds with the surrounding Si atoms, leading to the low density diamond structure. This structure limits the number of possible diffusion paths of point defects and/or impurity atoms to form pairs and in some cases also larger clusters. In the continuum description, isotropic diffusion is assumed for instance in the theory of diffusion-limited reactions of reacting particles in a solid [4]. In most cases an empirical value of the capture radius is used, which is usually assumed to be about one or two times the bond length of Si [5, 6] as this leads to a reasonable reproduction of the experimental observations.

Nowadays, molecular dynamics (MD) calculations are widely used to simulate atomistic phenomena and are often regarded as a virtual experiment. MD calculations are useful in showing an atomistic phenomenon visually. One of the tough points for "virtual" experimentalists is, however, the inefficiency in calculating the physical or chemical process often requiring a lot of iterations and attempts as well as extensive calculation resources. For the reaction between two point defects, this includes a good understanding on an atomistic scale of the point defect diffusion and of the capture cross-section for the capture of one point defect by another one.

Estimating quantitatively the capture cross-section of a V for capturing another V thus forming a di-vacancy is our final goal. In the present paper, as a first step, the diffusion paths of two neighbouring vacancies in silicon are investigated. For this purpose, a program code was developed to determine all basic irreducible atomic configurations in the supercell for a given atomic defect concentration. To illustrate the application of this code, the possible diffusion paths leading to di-vacancy formation were studied using a 64-Si atoms supercell. The ground state of an isolated V will have a somewhat lower energy than that obtained in larger supercells due to the more pronounced Jahn–Teller effect in a larger supercell [7]. This, however, leads only to a shift of the reference energy when considering the binding between two vacancies and has a negligible or no impact on the most likely diffusion paths as was confirmed by a reference calculation on 216-Si atom supercell.

2 Calculation methods

2.1 Atomistic diffusion study All irreducible configurations of two vacancies in a 64-Si atom supercell are determined each with its weight (=the number of equivalent configurations) and this is done by considering the symmetry of the Si crystal and the periodic condition of the supercell. This search is performed automatically by using a script program code based on a published algorithm [8], and is similar to a method that has been used elsewhere [9]. The algorithm allows calculating all equivalent or so called irreducible configurations for any two substitutional point defects in a finite supercell together with the weight of each of these configurations. As an illustration, the algorithm is applied for two vacancies in a 64-atom supercell. The transition states (TS) searching is performed for all possible paths systematically connecting with the nearest neighbour sites.

It turns out that here are nine irreducible configurations of two vacancies in the 64-atom cell. Figure 1 shows these configurations, in which the white circles are the V positions and the other ones are Si atoms.

These nine configurations have been automatically extracted from the total number of 2016 ($=^{64}C_2$) configurations and form the basis for the further discussion. The total number of occurrences of each irreducible configuration (its "weight") is shown in Fig. 2 as a function of the nominal distance between the two vacancies. Here, each V position is defined by the position of the Si atom before removing it from the lattice and before the structural relaxation. The labels in Fig. 2 are showing the order of the nearest neighbors with respect to the fixed V at position #0. The 9th nearest neighbour position is the maximum distance from the vacancy at #0 within a 64-atom supercell. From the figure, it is clear that the positions labelled 2, 3, 6, and 7 have larger weights than the other ones and are thus more important when considering the dominant configurations for the diffusion of a V to the fixed one at #0, as discussed further.

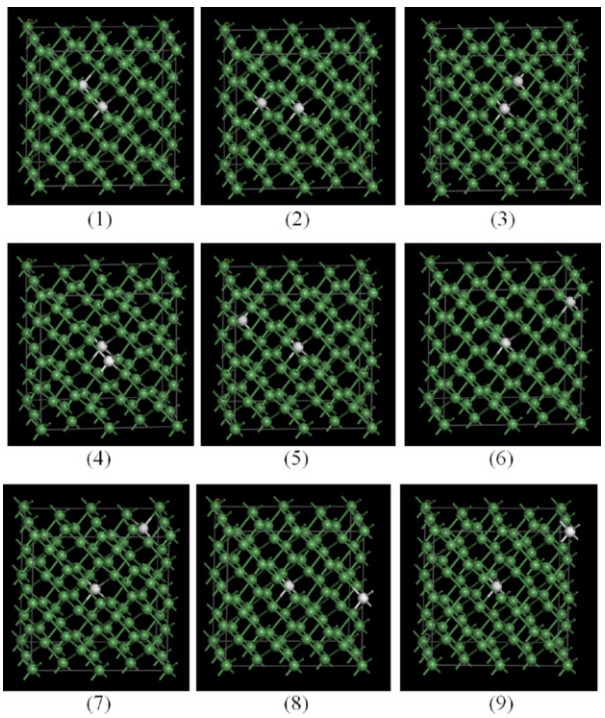

Figure 1 The nine basic configurations of two vacancies (in white) in a 64-Si atom cell.

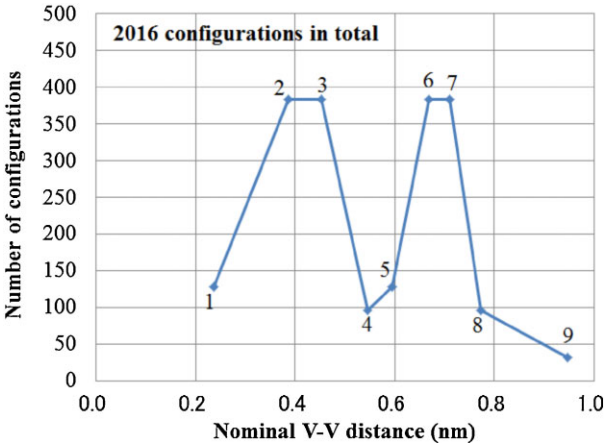

Figure 2 The weight for each V configuration as a function of the nominal distance to the second V which is assumed to be immobile. The labels are the order of the distance from 1st nearest neighbor to 9th nearest neighbor.

2.2 Basic calculation conditions The DFT calculations are based on the standard approach, using the local density approximation [10, 11] with the ultrasoft pseudopotential method [12], and plane waves as basis set for efficient structure optimization. The expression proposed by Perdew et al. [13] is used for the exchange-correlation energy in the generalized gradient approximation (GGA). The *CASTEP* code is used to self-consistently solve the Kohn–Sham equation using a three-dimensional periodic boundary condition [14]. The density mixing method [15] and the BFGS geometry optimization method [16] are used to optimize the electronic structure and the atomic configurations, respectively. Only the neutral charge state of the system is considered. For *k*-point sampling, the $2 \times 2 \times 2$ special points of the Monkhorst–Pack grid [17] are used. The cutoff energy of the plane waves is 350 eV. The diffusion barriers at the TS are estimated by the LST/QST method [18].

3 Results and discussion

3.1 Binding energies and barrier heights of transition states Cells with the nine basic configurations are relaxed and the transition states between two configurations are determined using the LST/QST method. Furthermore, the binding energy of the two vacancies is calculated for each configuration by using the formation energy of an isolated V which is 3.47 eV as calculated by the standard approach using the "self-energy" of a Si atom in the

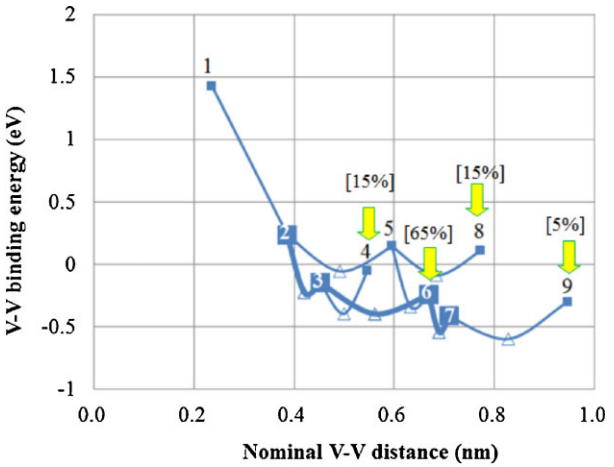

Figure 3 Binding energies for the nine basic configurations of two vacancies in a 64-atom supercell and for their transition states, whereby one V is assumed to be immobile. Atoms labelled #4, #6, #8, #9 are close to the boundary of the 64-atoms cell. There are no other paths for a moving V to approach the one at the position #0 (the center position of the 64-atoms cell). Numbers in brackets are the weight (in percent) of the different diffusion paths.

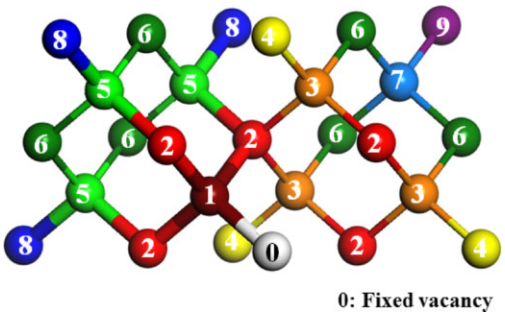

Figure 4 Configurations of two vacancies in a 64-atom cell supposing one V is fixed while the other one is migrating. Zigzag chains of Si atoms in ⟨110⟩ direction including the positions labelled #0 and #1 are shown with wider bonding sticks.

perfect cell. As expected, this value is somewhat below the 3.578 eV obtained in a previous study using a 216-atom cell [19].

Figure 3 shows the binding energy of the two vacancies as a function of the nominal distance between them. Although the formation energy of an isolated V in the 64-atom supercell used in the present study is somewhat different from that obtained in larger supercells, this difference only leads to a shift of the reference energy. In this figure, the binding energies at the transition states are also shown and represented by triangles. The most stable configuration is labelled #1, and is the one in which two vacancies are located at the nearest neighbour site, i.e., the di-vacancy. The obtained binding energy is 1.43 eV, which is lower than the 2 eV reported previously [20, 21] but close to the reported experimental values (1.5 eV [22], $\gtrsim$1.6 eV [23]). All the possible diffusion paths between the nine irreducible configurations shown in Fig. 1 are connected by the curves through their transition states. Actually, a transition state between #1 and #2 was not found so #2 is unstable and moves to #1. The possible paths for actual V diffusion are limited and go through the bond centered positions as shown by the curves in Fig. 3. Other directions have much higher diffusion barrier heights that are typically, larger than 3 eV. Exceptions are #2→#1 as mentioned above, a maximum of 0.343 eV in #4→#3 and a minimum of 0.076 eV in #3→#2.

3.2 Configurations of two vacancies The energetically most favorable path to form a di-vacancy is thus #8→#5→#2→#1 and therefore it is often assumed that this path is the only one to form the di-vacancy [24]. The diffusion paths of V are visualized in Fig. 4 showing the possible atomic configurations with one V fixed at the position #0 while the other numbers are the positions of the second V in the 64-atom supercell of Fig. 1. Diffusion of vacancies is accompanied by phonon vibration, and is the result of many attempts to cross the barrier, whereby the number of attempts needed increases with increasing barrier height. This vibration which is predicted in MD, however, makes it difficult to determine the dominant driving forces in the diffusion process.

The diffusion path #8→#5→#2→#1 follows one of the twelve zigzag Si chains along the ⟨110⟩ directions around the #0 V in Fig. 4. If V diffuses along this path, it can easily form a di-vacancy due to the low barrier height. MD calculations also found an attractive field created by a mono-vacancy on zigzag Si chains in silicon [25]. Among all the paths for the moving V to approach the #0 V, the diffusion path 8→#5→#2→#1 has, however, only a weight of 15%, while the other paths have together 85% weight and are not following the zigzag chains around #0, although these paths have about 0.3 eV higher diffusion barriers.

3.3 Continuum model versus atomistic picture In history of the science and technology, many phenomena have been understood and discussed by using continuum models due to a lack of atomistic models and calculation methods. Nowadays, ab initio calculations can be used to reveal the atomistic details and processes behind the continuum models and as illustrated in the present paper allow to calculate model parameter values rather than empirically choosing them. Using a 64-atom cell as in the present study has of course its limits and does not allow to investigate long-range interaction between two vacancies or point defects which is needed for a more accurate calculation of e.g., the capture cross-section. For that purpose larger cells have to be used. Figure 3, however, represents a new atomistic picture of the formation of a di-vacancy and, when used for a much larger supercell will allow also to calculate the effective capture cross-section that can be used in continuum models. The results of a detailed study using much larger supercells to estimate the capture cross-section for the formation of a di-vacancy in Si will be published

elsewhere [26]. Finally, it should also be noted that the weighed number of atoms on the twelve zigzag Si chains along the ⟨110⟩ directions around the #0 V will relatively decrease when considering a larger volume around the #0 V as will be the case for larger supercells.

4 Conclusion A method is proposed to investigate all possible diffusion paths for the formation of a point defect pair in Si based on an atomistic picture. Systematically calculating all of the irreducible configurations of two point defects including their weight is a first step towards the calculation of the effective capture cross-section. In the present paper, as an illustration, the diffusion paths for the capturing of a V by another V forming a di-vacancy are described. The energetically most favorable diffusion paths of V to form a di-vacancy are the twelve zigzag Si chains along ⟨110⟩ directions around the second V which is assumed to be immobile. Many more possible paths exist, however, having about 0.3 eV higher diffusion barriers. Taking into account the relative weight of the different possible diffusion paths, the atomistic picture obtained in the present study is a first step towards calculating the capture cross-section for pair formation.

Acknowledgements This work is partially supported by the Advanced Low Carbon Technology Research and Development Program (ALCA) of the Japan Science and Technology Agency (JST). We would like to thank Dr. Abhijit Chatterjee of Accelrys Software Inc., for stimulating discussions and for developing the script program code that is used in the present study to calculate the irreducible vacancy configurations. Mr. Matsutani of Okayama Prefectural University is acknowledged for figure preparation.

References

[1] M. Muranaka, K. Makabe, M. Miura, H. Kato, S. Ide, H. Iwai, M. Kawamura, Y. Tadaki, M. Ishihara, and T. Kaeriyama, Jpn. J. Appl. Phys., Part 1 **37**, 1240 (1998).
[2] H. Ishii, S. Shiratake, K. Oka, K. Motonami, T. Koyama, and J. Izumitani, Jpn. J. Appl. Phys., Part 2 **35**, L1385. (1996).
[3] M. Miyazaki, S. Miyazaki, T. Kitamura, Y. Yanase, T. Ochiai, and H. Tsuya, Jpn. J. Appl. Phys., Part 1 **36**, 6187. (1997).
[4] T. R. Waite, Phys. Rev. **107**, 463 (1957).
[5] M. Mikelsen, E. V. Monakhov, G. Alfieri, B. S. Avset, and B. G. Svensson, Phys. Rev. B **72**, 195207 (2005).
[6] G. D. Watkins, J. Appl. Phys. **103**, 106106 (2008).
[7] M. J. Puska, S. Pöykkö, M. Pesola, and R. M. Nieminen, Phys. Rev. B **58**, 1318 (1998).
[8] J. L. Gavartin, M. Sarwar, D. C. Papageorgopoulos, D. Gunn, S. Garcia, A. Perlov, A. Krzystala, D. L. Ormsby, D. Thompsett, G. Goldbeck-Wood, A. Andersen, and S. French, ECS Trans. **25**, 1335 (2009).
[9] R. Grau-Crespo, S. Hamad, C. R. A. Catlow, and N. H. de Leeuw, J. Phys.: Condens. Matter **19**, 256201 (2007).
[10] P. Hohenberg and W. Kohn, Phys. Rev. **136**, B864 (1964).
[11] W. Kohn and L. Sham, Phys. Rev. **140**, A1133 (1965).
[12] D. Vanderbilt, Phys. Rev. B **41**, 7892 (1990).
[13] J. P. Perdew, K. Burke, and M. Ernzerhof, Phys. Rev. Lett. **77**, 3865 (1996).
[14] The CASTEP code is available from Accelrys Software Inc.
[15] G. Kresse and J. Furthmüller, Phys. Rev. B **54**, 11169 (1996).
[16] T. Fischer and J. Almlof, J. Phys. Chem. **96**, 9768 (1992).
[17] H. Monkhorst and J. Pack, Phys. Rev. B **13**, 5188 (1976).
[18] N. Govind, M. Petersen, G. Fitzgerald, D. King-Smith, and J. Andzelm, Comput. Mater. Sci. **28**, 250 (2003).
[19] K. Sueoka, E. Kamiyama, and J. Vanhellemont, J. Appl. Phys. **114**, 153510 (2013).
[20] H. Seong and L. J. Lewis, Phys. Rev. B **53**, 9791 (1996).
[21] D. V. Makhov and J. L. Lewis, Phys. Rev. Lett. **92**, 255504 (2004).
[22] J. W. Corbett, Electron Radiation Damage in Semiconductors and Metals (Academic, New York, 1996), and references therein.
[23] G. D. Watkins and J. W. Corbett, Phys. Rev. **138**, A543 (1965).
[24] G. S. Hwang and W. A. Goddard, III, Phys. Rev. B **65**, 233205 (2002).
[25] A. Bongiorno and L. Colombo, Phys. Rev. B **57**, 8767 (1998).
[26] E. Kamiyama, J. Vanhellemont, and K. Sueoka, to be submitted for publication in J. Appl. Phys.

